

## Supporting Information

# Field-induced Slow Magnetic Relaxation of a Six-Coordinate Mononuclear Manganese(II) and Cobalt(II) Oxamate Complexes

*Tamyris T. da Cunha*<sup>‡,†</sup> *Vitor M. M. Barbosa*,<sup>†</sup> *Willian X. C. Oliveira*,<sup>†</sup> *Emerson F.*

*Pedroso*,<sup>‡</sup> *Diana M. A. García*,<sup>§</sup> *Wallace C. Nunes*,<sup>§</sup> *Cynthia L. M. Pereira*<sup>\*,†</sup>

<sup>‡</sup>Instituto Federal de Educação, Ciência e Tecnologia de Minas Gerais, Campus Avançado Itabirito. R. José Benedito, 139, Santa Efigênia, Itabirito, MG, 35450-000, Brazil.

<sup>†</sup>Departamento de Química, Instituto de Ciências Exatas, Universidade Federal de Minas Gerais. Av. Antônio Carlos 6627, Pampulha, BH, MG, 31270-901 Brazil. e-mail: [cynthialopes@ufmg.br](mailto:cynthialopes@ufmg.br)

<sup>‡</sup>Centro Federal de Educação Tecnológica de Minas Gerais, Av. Amazonas 5523, BH, MG, 30421-169, Brazil.

<sup>§</sup>Instituto de Física, Universidade Federal Fluminense, Av. Gal. Milton Tavares de Souza, s/nº, Campus da Praia Vermelha, 24210-346, Niterói, RJ, Brazil.

**Keywords:** oxamate; cobalt; manganese; magnetism; single-molecule magnet.

## EXPERIMENTAL SECTION

**Material and Methods.** All chemicals and solvents used were of analytical grade and used without further purification. The ligand 4-HOpa [4-HOpa = (4-hydroxyphenyl)oxamate] was synthesized according to the literature methods.<sup>1</sup> Elemental analyses (C, H, and N) were performed using a Perkin-Elmer 2400 analyzer and the atomic absorption for Mn and Co were carried out with a Hitachi Z-8200 Polarized Atomic Absorption Spectrophotometer. Infrared spectra were recorded on a Perkin Elmer 882 Spectrophotometer in the range 4000 and 400  $\text{cm}^{-1}$  using dry KBr pellets. Thermogravimetric analysis (TG/DTA) data were collected with a Shimadzu TG/DTA 60 under a nitrogen atmosphere at a heating rate of 10  $^{\circ}\text{C min}^{-1}$  from room temperature to 750  $^{\circ}\text{C}$ . Powder X-ray diffraction patterns (PXRD) were obtained from a Shimadzu XRD-7000 X-RAY by using  $\text{Cu-K}\alpha_1$  radiation. DC magnetic measurements were performed in polycrystalline samples of **1** and **2**, using a Cryogenics SQUID magnetometer model S700. The magnetization curves at different temperatures for Mn complex were measured using a Quantum Design MPMS 3 SQUID-VSM (UFRJ, Brazil). Diamagnetism of the sample and the sample holder were taken into account. AC magnetic measurements were done by using a Quantum Design PPMS. Both ac and dc magnetic measurements were performed in samples placed in gelatin capsules with mineral oil to prevent crystals movement.

### Synthesis of the compounds

Synthesis of  $[\text{Mn}(\text{4-HOpa})_2(\text{H}_2\text{O})_2]$  (**1**): 1.0 mmol (0.203 g) of 4-HOpa were dissolved in 25 mL of  $\text{H}_2\text{O}$  while stirring to produce a colorless solution. A solution containing 0.5 mmol (0.099 g) of  $\text{MnCl}_2 \cdot 4\text{H}_2\text{O}$  in  $\text{H}_2\text{O}$  (25 mL) was slowly added. The resulting colorless solution was stirred for 15 min while being heated to 60 °C. The solution was left to cool and crystallize. Colorless prismatic crystals were obtained after 2 days. Yield: 67% (0.151 g). Selected IR peaks ( $\text{cm}^{-1}$ ): 3386 (s), 3332 (s), 1644 (s), 1552 (s), 1512 (s), 1360 (m), 1252 (m), 832 (m), 806 (m). Elemental analysis calcd (%) for  $\text{C}_{16}\text{H}_{16}\text{MnN}_2\text{O}_{10}$ : C 42.59, H 3.57, N 6.21, Mn 12.17; found C 42.85, H 3.63, N 6.35, Mn 12.64%.

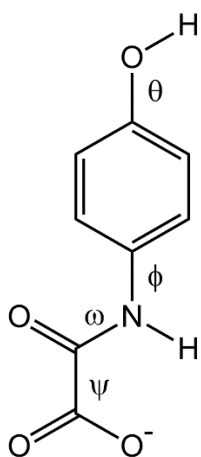
Synthesis of  $[\text{Co}(\text{4-HOpa})_2(\text{H}_2\text{O})_2]$  (**2**): 1.0 mmol (0.203 g) of 4-HOpa were dissolved in 25 mL of  $\text{H}_2\text{O}$  while stirring to produce a colorless solution. A solution containing 0.5 mmol (0.182 g) of  $\text{Co}(\text{ClO}_4)_2 \cdot 6\text{H}_2\text{O}$  in  $\text{H}_2\text{O}$  (25 mL) was slowly added. The resulting light pink solution was stirred for 15 min while being heated to 60 °C. The solution was left to cool and crystallize. Light pink prismatic crystals were obtained after 2 days. Yield: 73% (0.166 g). Selected IR peaks ( $\text{cm}^{-1}$ ): 3338 (s), 3308 (s), 1646 (s), 1556 (m), 1512 (m), 1360 (m), 1254 (m), 836 (m), 808 (m). Elemental analysis calcd (%) for  $\text{C}_{16}\text{H}_{16}\text{CoN}_2\text{O}_{10}$ : C 42.21, H 3.54, N 6.15, Co 12.95; found C 41.92, H 3.14, N 6.15, Co 13.54%.

### **X-ray Crystal Structure Analysis**

X-ray diffraction data for **1** and **2** were performed with an Oxford-Diffraction GEMINI-Ultra diffractometer using Enhance Source Mo- $K_{\alpha}$  radiation ( $\lambda = 0.71073 \text{ \AA}$ ). Measurements were performed at different temperatures, as shown in Table S1. Data integration and scaling of the reflections for all compounds were performed with the *CRYSTALIS* suite.<sup>2</sup> Final unit cell parameters were based on the fitting of the positions of all reflections. Analytical absorption corrections were performed by means of the *CRYSTALIS* suite, and the space group identification was done with *XPREP*.<sup>3</sup> The structures of all compounds were solved by direct methods using *SUPERFLIP*<sup>4,5</sup> or *SIR-92*<sup>6</sup> programs. For each compound, the positions of all non-hydrogen atoms could be unambiguously assigned on consecutive difference Fourier maps. Refinements were performed using *SHELXL*<sup>7</sup> based on  $F^2$  through the full-matrix least-squares routine. All non-hydrogen atoms were refined with anisotropic atomic displacement parameters. The hydrogen atoms were located in difference maps and included as fixed contributions according to the riding model. For water molecules, the distance O–H was fixed to 0.90  $\text{\AA}$  and  $U_{\text{iso}}(\text{H}) = 1.5 U_{\text{eq}}(\text{O})$ . The values of C–H and N–H of the organic moieties were considered equal to 0.97  $\text{\AA}$  and  $U_{\text{iso}}(\text{H}) = 1.2 U_{\text{eq}}(\text{C or N})$ .<sup>8</sup> A double split position model was applied to model disordered aromatic carbon atoms in **1** and **2**. Atomic coordinates, thermal parameters, bond lengths, and angles have been deposited at the Cambridge Crystallographic Data Centre (CCDC). Any request to the CCDC for this material should quote the full literature citation and the reference numbers CCDC 2006218 (**1**) and 2006217 (**2**).

## TORSION ANGLES

The torsion angles (see scheme 1)  $\psi$  around the C–C oxamate bond are very low in both structures, equal to  $1.9^\circ$  for **1** and  $2.8^\circ$  for **2**, probably because of the bidentate coordination mode. The torsion angle  $\omega$  around C–N amide group is equal to  $4.4^\circ$  for **1** and  $5.5^\circ$  for **2**, and the aromatic carbon amide angle  $\phi$  can vary from  $24.1^\circ$  to  $50.5^\circ$  and  $20.1^\circ$  to  $48.8^\circ$  for **1** and **2**, respectively, due to the disorder present in the aromatic ring. Finally, considering the phenol C–O torsion angle  $\theta$ , it can vary much less, from  $2.2^\circ$  to  $4.9^\circ$  for **1** and  $3.0^\circ$  for **2**, probably to keep the hydrogen bond distances and thus the hydrogen bond independent of the phenol ring torsion angles. An overlay between the crystal structures **1** and **2** is shown in Figure S3.



**Scheme 1.** General scheme of the ligand 4-HOpa showing the notation used to describe the torsion angles for **1** and **2**.

**Table S1.** Summary of the crystal data and refinement parameters for **1-2**.

Compound	1	2
Chemical Formulae	C <sub>16</sub> H <sub>16</sub> N <sub>2</sub> O <sub>10</sub> Mn	C <sub>16</sub> H <sub>16</sub> N <sub>2</sub> O <sub>10</sub> Co
<i>F</i> w / g mol <sup>-1</sup>	451.25	455.24
$\lambda$ / Å	0.71073	0.71073
Crystal Size / mm <sup>3</sup>	0.87 × 0.62 × 0.17	0.17 × 0.10 × 0.08
Crystal System	Monoclinic	Monoclinic
Space Group	<i>C</i> 2/ <i>c</i>	<i>C</i> 2/ <i>c</i>
<i>a</i> / Å	13.9234(4)	13.7192(5)
<i>b</i> / Å	6.4958(2)	6.3594(2)
<i>c</i> / Å	20.0347(6)	20.1235(8)
$\alpha$ / °	90	90
$\beta$ / °	105.061(3)	105.011(4)
$\gamma$ / °	90	90
Volume / Å <sup>3</sup>	1749.77(9)	1695.78(11)
<i>T</i> / K	298(2)	150(2)
<i>Z</i>	4	4
<i>F</i> (000)	924	932
<i>hkl</i> range	-21 ≤ <i>h</i> ≤ 20 -9 ≤ <i>k</i> ≤ 9 -30 ≤ <i>l</i> ≤ 29	-18 ≤ <i>h</i> ≤ 17 -8 ≤ <i>k</i> ≤ 8 -25 ≤ <i>l</i> ≤ 25
$\rho_{\text{calc}}$ / g cm <sup>-3</sup>	1.713	1.783
$\mu$ / mm <sup>-1</sup>	0.818	1.078
Collected reflections	18442	13784
Independent Reflections	3082	2199
Reflections with $I \geq 2\sigma(I)$	2737	1952
<i>R</i> <sub>int</sub>	0.0286	0.0338
<i>R</i> <sup>a</sup> ; <i>wR</i> <sup>b</sup> [ $I \geq 2\sigma(I)$ ]	0.0292; 0.0783	0.0257; 0.0600
<i>R</i> <sup>a</sup> ; <i>wR</i> <sup>b</sup> (all data)	0.0340; 0.0824	0.0312; 0.0635
Goodness-of-fit on <i>F</i> <sup>2</sup> ( <i>S</i> <sup>c</sup> )	1.088	1.032
Larg. diff. peak and hole/e Å <sup>-3</sup>	+0.303; -0.340	+0.442; -0.336
CCDC	2006218	2006217

<sup>a</sup>  $R = \sum ||F_o| - |F_c|| / \sum |F_o|$ . <sup>b</sup>  $wR = [\sum w(|F_o|^2 - |F_c|^2)^2 / \sum w|F_o|^2]^{1/2}$ . <sup>c</sup>  $S = [\sum w(|F_o|^2 - |F_c|^2)^2 / (N_o - N_p)]^{1/2}$  where *w* is proportional to  $\sigma^{-1}$  whereas *N*<sub>o</sub> and *N*<sub>p</sub> are the number of observed and refined parameters, respectively.

**Table S2.** Geometry of hydrogen bonds present in the crystal packing of **1**.

		Distance / Å		Angle / °
D—H···A	D—H	H···A	D···A	D—H···A
O5—H5A···O4 <sup>i</sup>	0.90	1.991	2.849(9)	158.2
O4 <sup>ii</sup> —H4 <sup>ii</sup> ···O1	0.82	1.805	2.595(9)	161.3
O5—H5B···O2 <sup>iii</sup>	0.90	1.877	2.756(1)	165.1

Symmetry codes: (i)  $x, 1+y, z$ ; (ii)  $\frac{1}{2}+x, 1.5-y, \frac{1}{2}+z$ , (iii)  $\frac{1}{2}+x, \frac{1}{2}-y, \frac{1}{2}+z$ .

**Table S3.** The geometry of hydrogen bonds present in the crystal packing of **2**.

		Distance / Å		Angle / °
D—H···A	D—H	H···A	D···A	D—H···A
O5—H5A···O4 <sup>i</sup>	0.90	1.91	2.751(2)	155.0
O4 <sup>ii</sup> —H4 <sup>ii</sup> ···O1	0.82	1.87	2.667(1)	162.2
O5—H5B···O2 <sup>iii</sup>	0.90	1.85	2.726(1)	164.7

Symmetry codes: (i)  $-1+x, 1+y, z$ ; (ii)  $2-x, 2-y, -z$ ; (iii)  $x, 2+y, -1+z$ ; (iv)  $x, -1+y, +z$ .

**Table S4.** Best fitting parameters for **1** measured under the dc field of 1.0 kOe.

T / K	$\chi_s / \text{cm}^3 \text{K mol}^{-1}$	$\chi_T / \text{cm}^3 \text{K mol}^{-1}$	$\alpha$	$\tau / \text{s}$
2.0	1.204(6)	2.05(8)	0.42(3)	1.75(4) x10 <sup>-2</sup>
2.2	1.081(6)	1.79(4)	0.339(28)	8.13(11) x10 <sup>-3</sup>
2.4	1.000(8)	1.59(3)	0.24(4)	4.7(5) x10 <sup>-3</sup>
2.6	0.925(6)	1.62(3)	0.32(2)	7.0(8) x10 <sup>-3</sup>
2.8	0.867(2)	1.548(11)	0.279(8)	5.7(2) x10 <sup>-3</sup>
3.0	0.807(2)	1.467(9)	0.259(9)	4.86(15) x10 <sup>-3</sup>
3.2	0.759(2)	1.419(7)	0.2417	4.50(10) x10 <sup>-3</sup>
3.4	0.713(2)	1.345(6)	0.216(7)	3.86(7) x10 <sup>-3</sup>
3.6	0.658(4)	1.26(61)	0.199(16)	3.21(13) x10 <sup>-3</sup>
3.8	0.623(2)	1.233(7)	0.197(10)	3.00(13) x10 <sup>-3</sup>
4.0	0.592(2)	1.172(7)	0.196(10)	3.0(7) x10 <sup>-3</sup>
4.2	0.565(4)	1.098(10)	0.186(18)	2.61(10) x10 <sup>-3</sup>
4.4	0.539(2)	1.044(4)	0.158(9)	2.37(4) x10 <sup>-3</sup>
4.6	0.5176(16)	1.014(4)	0.163(7)	2.26(3) x10 <sup>-3</sup>
4.8	0.4974(19)	0.986(4)	0.162(9)	2.18(4) x10 <sup>-3</sup>
5.0	0.4777(15)	0.948(3)	0.162(7)	2.02(3) x10 <sup>-3</sup>
5.5	0.436(4)	0.857(7)	0.131(19)	1.62(6) x10 <sup>-3</sup>
6.0	0.401(3)	0.798(4)	0.138(13)	1.47(4) x10 <sup>-3</sup>
6.5	0.369(3)	0.751(4)	0.154(13)	1.36(3) x10 <sup>-3</sup>
7.0	0.3452(19)	0.689(3)	0.129(11)	1.17(2) x10 <sup>-3</sup>
7.5	0.321(4)	0.630(6)	0.108(26)	9.8(4) x10 <sup>-4</sup>
8.0	0.301(2)	0.596(3)	0.120(13)	9.18(21) x10 <sup>-4</sup>
8.5	0.281(2)	0.579(3)	0.156(13)	9.07(23) x10 <sup>-4</sup>
9.0	0.266(4)	0.529(5)	0.117(24)	7.5(3) x10 <sup>-4</sup>
9.5	0.252(2)	0.520(3)	0.142(15)	7.5(2) x10 <sup>-4</sup>
10.0	0.240(2)	0.491(2)	0.138(14)	6.78(18) x10 <sup>-4</sup>
11.0	0.218(2)	0.4407(18)	0.120(13)	5.64(13) x10 <sup>-4</sup>
12.0	0.200(2)	0.401(3)	0.092(23)	4.74(19) x10 <sup>-4</sup>
13.0	0.187(4)	0.127(30)	0.127(30)	1.4(2) x10 <sup>-4</sup>
14.0	0.1719(35)	0.14(3)	0.14(3)	3.75(19) x10 <sup>-4</sup>

**Table S5.** Best fitting parameters for **2** measured under the dc field of 1.0 kOe.

T / K	$\chi_s / \text{cm}^3 \text{ K mol}^{-1}$	$\chi_T / \text{cm}^3 \text{ K mol}^{-1}$	$\alpha$	$\tau / \text{s}$
2.0	0.1465(6)	1.07(4)	0.24(2)	0.010(1)
2.2	0.135(5)	1.04(3)	0.22(2)	0.0090(6)
2.5	0.121(3)	0.89(1)	0.21(1)	0.0059(2)
3.0	0.102(3)	0.81(1)	0.21(1)	0.0046(1)
3.5	0.085(5)	0.737(2)	0.21(2)	0.0036(2)
4.0	0.076(5)	0.667(13)	0.22(2)	0.0025(1)
5.0	0.067(2)	0.536(3)	0.142(8)	0.00116(2)
6.0	0.058(6)	0.439(6)	0.09(2)	4.6(2)x10 <sup>-4</sup>
7.0	0.54(3)	0.386(2)	0.056(1)	1.99(4) x10 <sup>-4</sup>
9.0	0.047(7)	0.298(2)	0.028(2)	4.3(2)x10 <sup>-4</sup>
10.0	0.052(6)	0.274(1)	0.020(1)	2.32(7)x10 <sup>-5</sup>
11.0	0.04(5)	0.253(2)	0.07(8)	1.1(3)x10 <sup>-5</sup>
12.0	0.03(7)	0.228(1)	0.06(7)	6(3)x10 <sup>-6</sup>
13.0	0.04(12)	0.2116(7)	0.06(7)	3(2)x10 <sup>-6</sup>
14.0	0.1(4)	0.1967(9)	0.1(2)	1.8(7)x10 <sup>-6</sup>

**Table S6.** Best fitting parameters for **1** measured under the dc field of 1.5 kOe.

T / K	$\chi_s / \text{cm}^3 \text{ K mol}^{-1}$	$\chi_T / \text{cm}^3 \text{ K mol}^{-1}$	$\alpha$	$\tau / \text{s}$
2.0	0.004(9)	4.06(43)	0.49(50)	1.0(9) x10 <sup>-2</sup>
2.2	0.66(9)	1.35(7)	0.39(50)	8(2) x10 <sup>-3</sup>
2.5	0.60(5)	1.30(3)	0.30(20)	6.0(5) x10 <sup>-3</sup>
3.0	0.50(5)	1.46(3)	0.31(2)	8.0(7) x10 <sup>-3</sup>
3.5	0.43(5)	1.18(1)	0.18(1)	4.0(2) x10 <sup>-3</sup>
3.7	0.40(5)	1.17(2)	0.21(2)	4.0(2) x10 <sup>-3</sup>
4.0	0.38(4)	1.12(1)	0.17(1)	3.0(1) x10 <sup>-3</sup>
4.3	0.35(4)	1.13(1)	0.20(1)	4.0(1) x10 <sup>-3</sup>
4.5	0.32(5)	1.08(1)	0.20(2)	3.0(1) x10 <sup>-3</sup>
4.7	0.31(7)	1.02(2)	0.19(2)	3.0(2) x10 <sup>-3</sup>
5.0	0.303(5)	0.93(1)	0.14(2)	2.0(1) x10 <sup>-3</sup>
5.5	0.265(8)	0.89(2)	0.22(3)	3.0(2) x10 <sup>-3</sup>
6.0	0.251(3)	0.79(1)	0.13(1)	2.0(4) x10 <sup>-5</sup>
6.5	0.230(3)	0.75(1)	0.15(1)	2.0(4) x10 <sup>-3</sup>
7.0	0.216(5)	0.67(1)	0.11(2)	100(6) x10 <sup>-3</sup>
7.5	0.114(5)	0.39(1)	0.17(3)	58(3) x10 <sup>-3</sup>
8.0	0.118(6)	0.62(1)	0.12(3)	1.0(7) x10 <sup>-3</sup>
8.5	0.117(7)	0.55(1)	0.09(4)	1.0(7) x10 <sup>-3</sup>
9.0	0.168(5)	0.54(7)	0.11(3)	1.0(5) x10 <sup>-3</sup>
10.0	0.152(5)	0.47(1)	0.07(3)	8.1(4) x10 <sup>-4</sup>
11.0	0.136(7)	0.44(1)	0.10(4)	7.5(5) x10 <sup>-4</sup>
12.0	0.124(7)	0.42(1)	0.13(4)	6.6(5) x10 <sup>-4</sup>
13.0	0.117(5)	0.36(1)	0.06(3)	5.2(3) x10 <sup>-4</sup>
14.0	0.110(2)	0.31(1)	0.00(4)	3.0(5) x10 <sup>-4</sup>
15.0	0.104(2)	0.30(2)	0.00(1)	2.6(5) x10 <sup>-4</sup>
16.0	0.09(6)	0.30(5)	0.05(4)	3.2(2) x10 <sup>-4</sup>
17.0	0.09(12)	0.28(9)	0.06(9)	3.0(3) x10 <sup>-4</sup>
18.0	0.07(1)	0.29(9)	0.19(7)	3.0(4) x10 <sup>-4</sup>
19.0	0.08(8)	0.26(6)	0.10(6)	2.4(2) x10 <sup>-4</sup>
20.0	0.07(7)	0.25(4)	0.11(5)	2.1(2) x10 <sup>-4</sup>

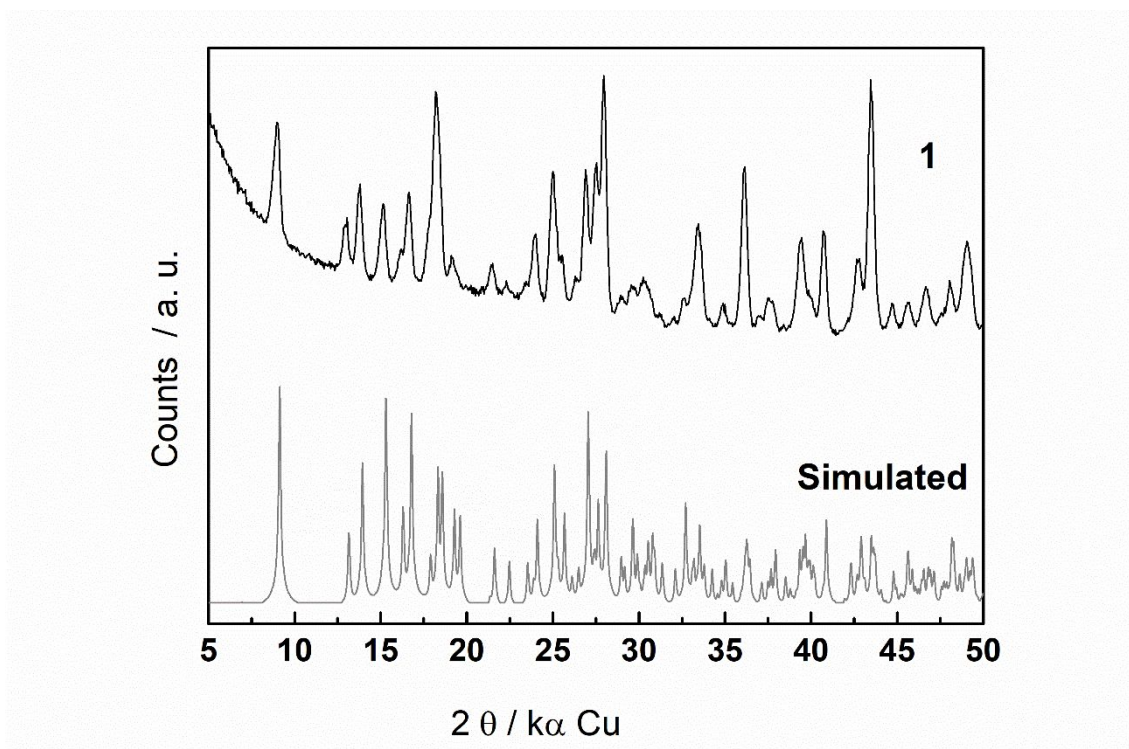


**Figure S1.** Powder X-ray diffraction patterns (PXR) of polycrystalline sample simulated using the Mercury program<sup>9</sup> (gray line) and experimental data (black line) of **1**.

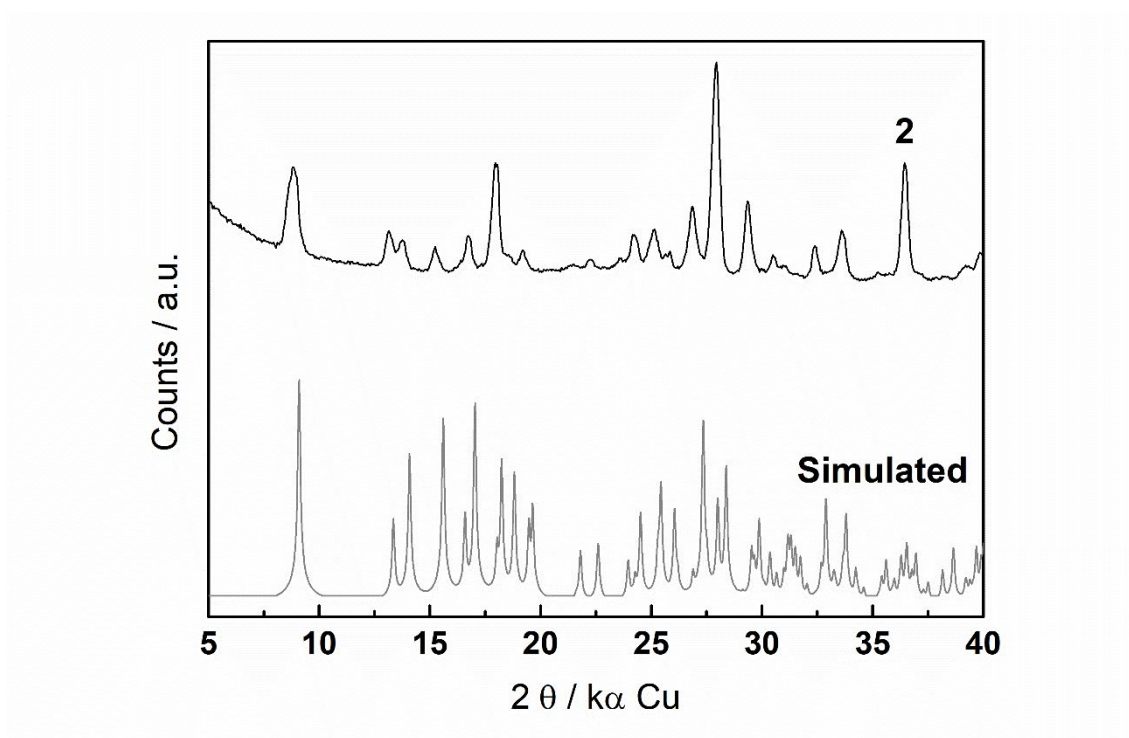


**Figure S2.** Powder X-ray diffraction patterns (PXR) of polycrystalline samples simulated using the Mercury program<sup>9</sup> (gray line) and experimental data (black line) of **2**.

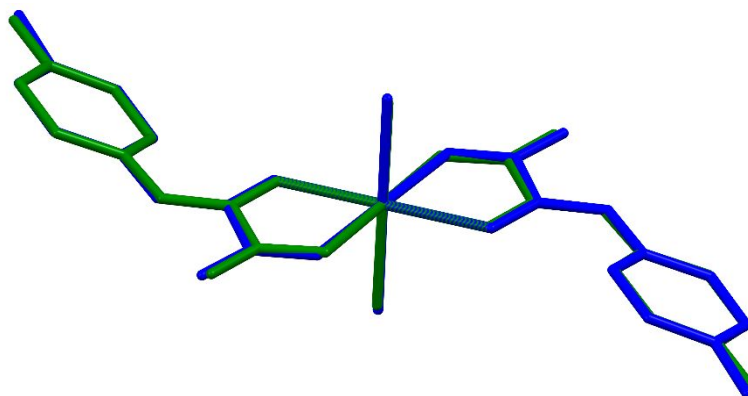
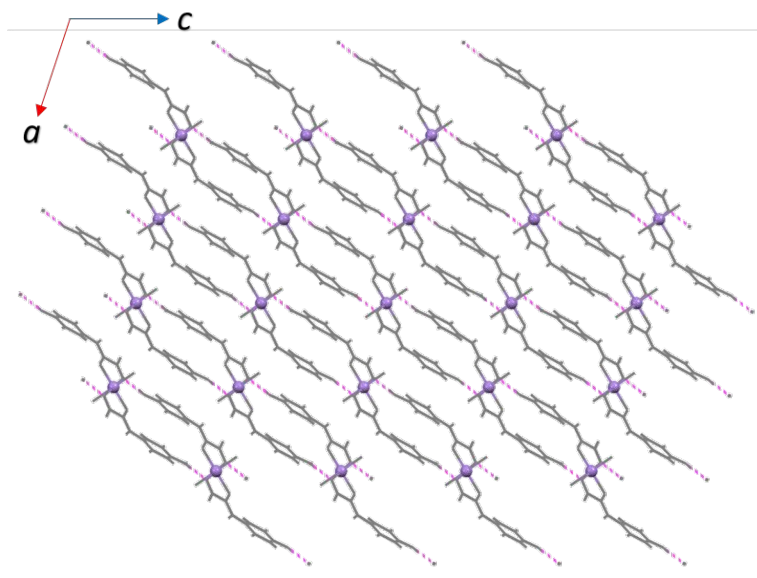


**Figure S3.** Overlay of crystal structures of **1** (in green) and **2** (in blue), featuring the small deviations on all but hydrogen atom positions. Metal atom's positions were merged for a better view. The average deviation of all atoms to its correspondent in the other structure is equal to 0.0577 Å. This RMS value was calculated by using the Mercury program according to the expression  $RMS = \sum_{i=1}^n \frac{1}{n} \sqrt{[\mathbf{r}_i^{Co} - \mathbf{r}_i^{Mn}]^2}$ , in which

$\mathbf{r}_i^{Co}$  = atomic position in  $\text{Co}(4\text{-HOpa})_2(\text{H}_2\text{O})_2$  structure;  $\mathbf{r}_i^{Mn}$  = atomic position in  $\text{Mn}(4\text{OHpa})_2(\text{H}_2\text{O})_2$  structure;  $n$  = total of non-hydrogen atoms in the asymmetric unit.

(a)



(b)

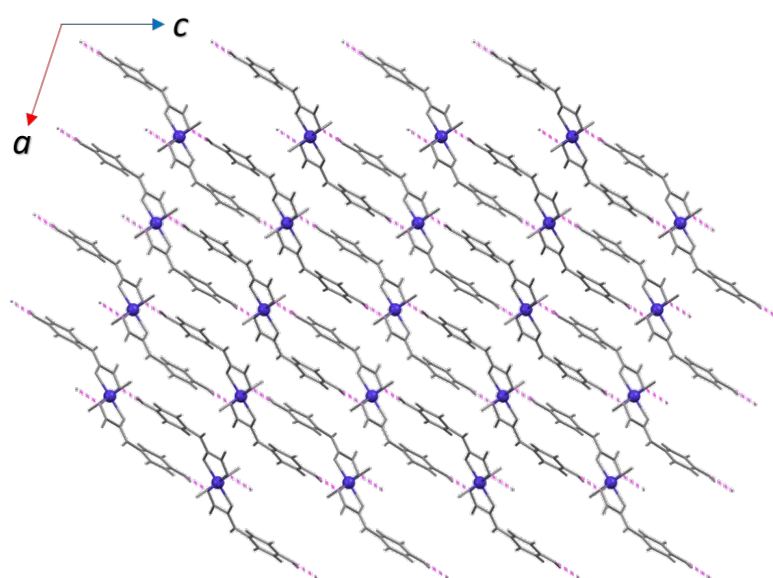
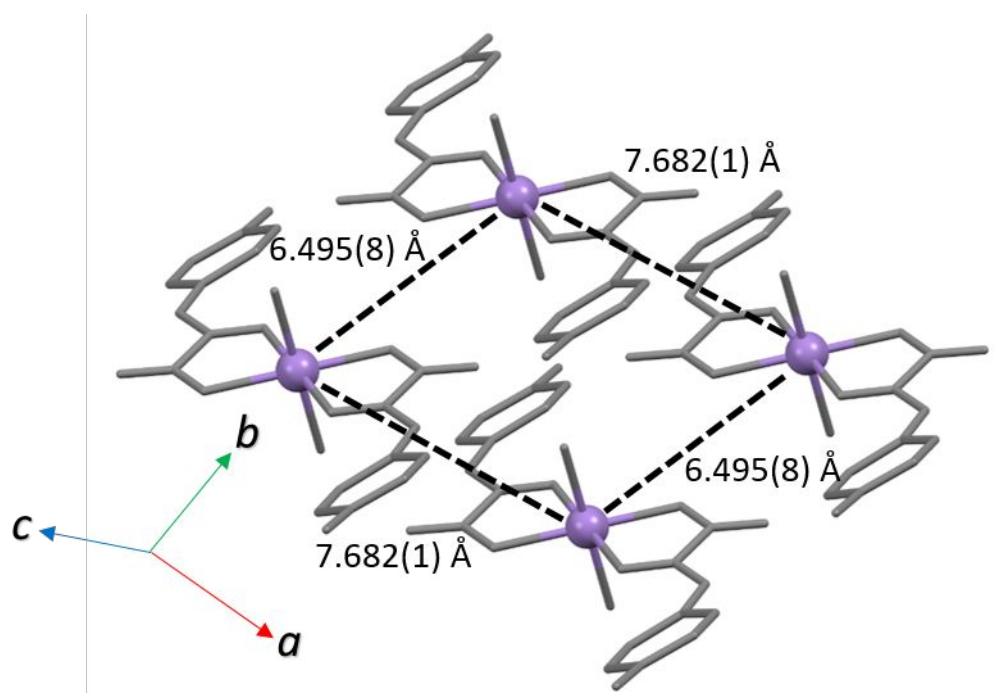


**Figure S4.** Representation of hydrogen bond pattern (dashed in pink) of (a) **1** and (b) **2** along *b* axis.

(a)



(b)

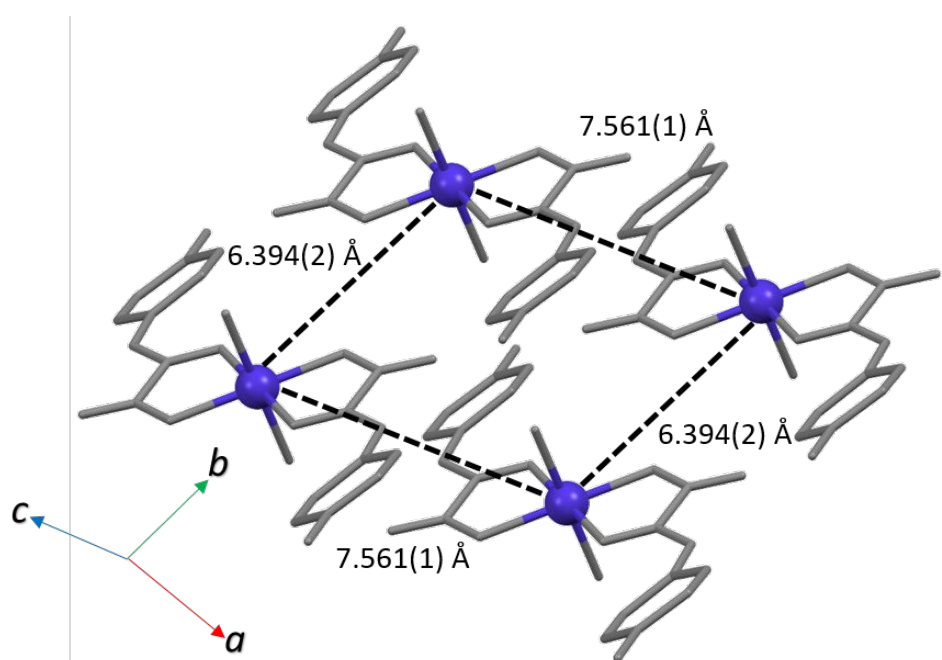


**Figure S5.** Representation of (a) Mn···Mn and (b) Co···Co distances between adjacent species in **1** and **2**, respectively. Atoms of manganese in purple, cobalt in the blue, intermetallic distance as dashed lines, other parts in gray and hydrogen atoms omitted for clarity.

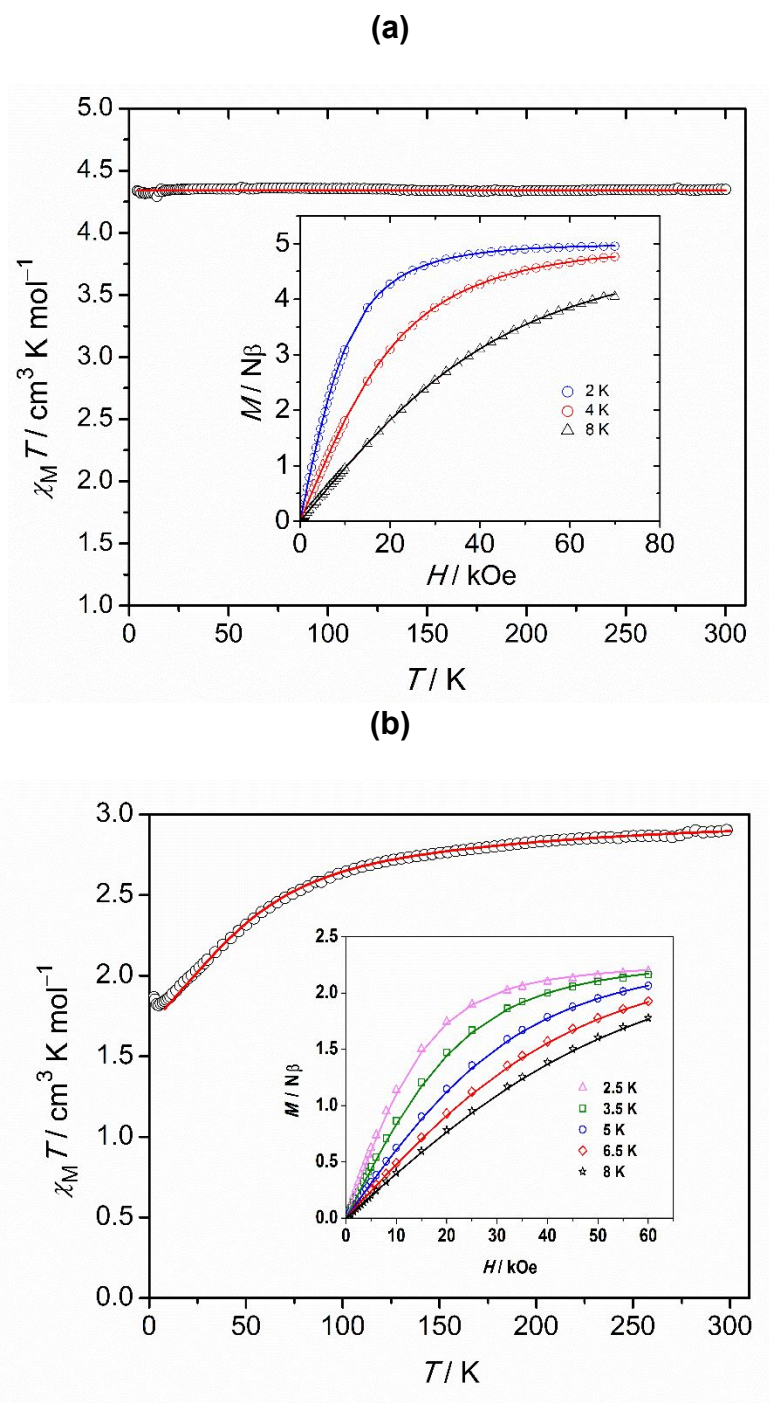
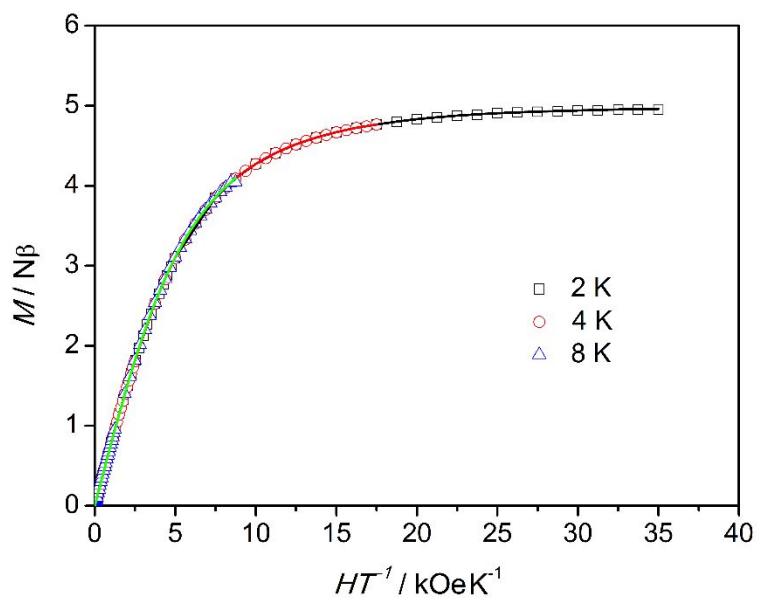


**Figure S6.** Magnetic data under the DC field for **1** (a) and **2** (b).  $\chi_M T$  vs  $T$  plot with  $H=200$  Oe. Symbols represent the experimental points, while solid lines correspond to the best-fit curves. Inset:  $M$  vs  $H$  plots at several temperatures for **1** and **2**. The agreement factor  $R$  between the experimental (exp) and calculated (calc)  $\chi_M T$  vs  $T$  and  $M$  vs  $H$  curves is defined by  $\Sigma[(\text{calc}) - (\text{exp})]^2 / (\text{exp})^2$  in the simultaneous fittings. We found  $R$  equal to  $3.64 \times 10^{-6}$  (**1**) and  $2.4 \times 10^{-5}$  (**2**).

(a)



(b)

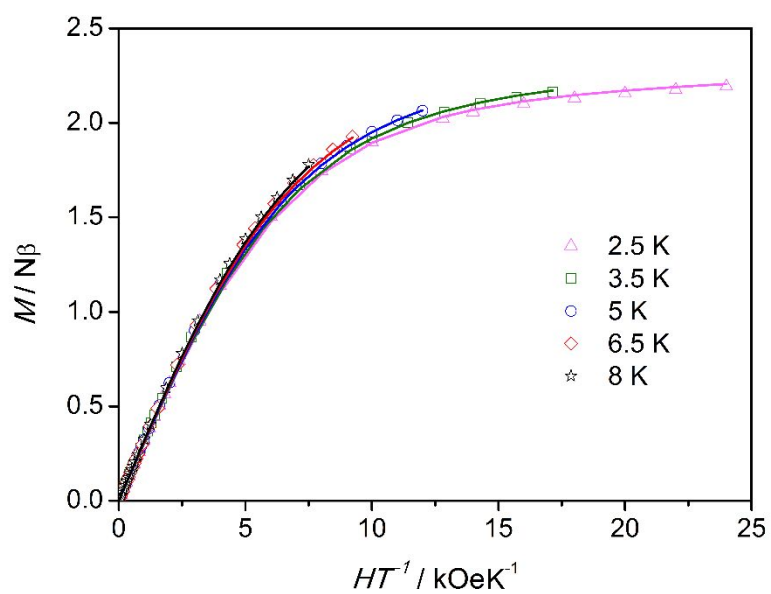


**Figure S7.** The reduced magnetization of **1** (a) and **2** (b) measured at several temperatures. Colored balls represent experimental points, while solid lines correspond to the simultaneous best-fit curves.

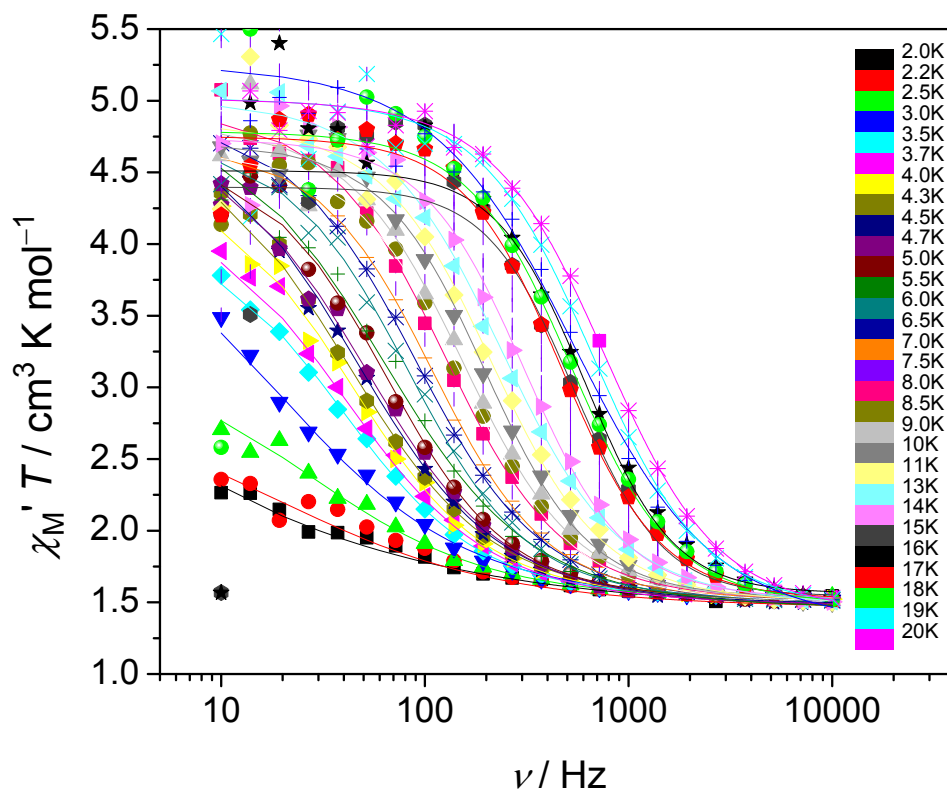


**Figure S8.**  $\chi_M' T$  vs.  $T$  curves for **1** from 20 K to 2.0 K.  $H_{dc} = 1.5$  kOe and frequency range from 10 Hz to 10 kHz. Solid lines correspond to the best-fit curves according to the generalized Debye model.

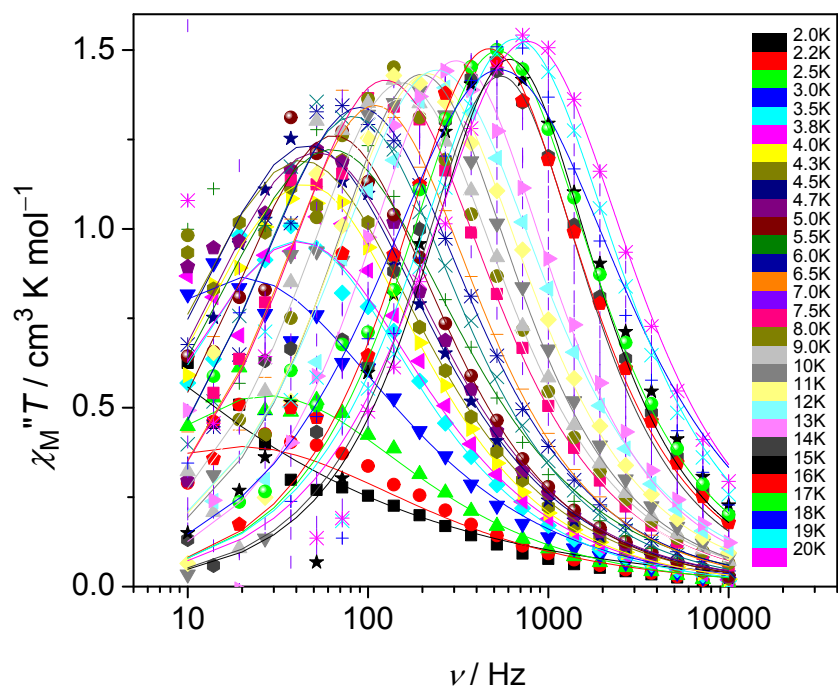


**Figure S9.**  $\chi_M'' T$  vs.  $T$  curves for **1** from 20 K to 2.0 K.  $H_{dc} = 1.5$  kOe frequency range from 10 Hz to 10 kHz. Solid lines correspond to the best-fit curves according to the generalized Debye model.

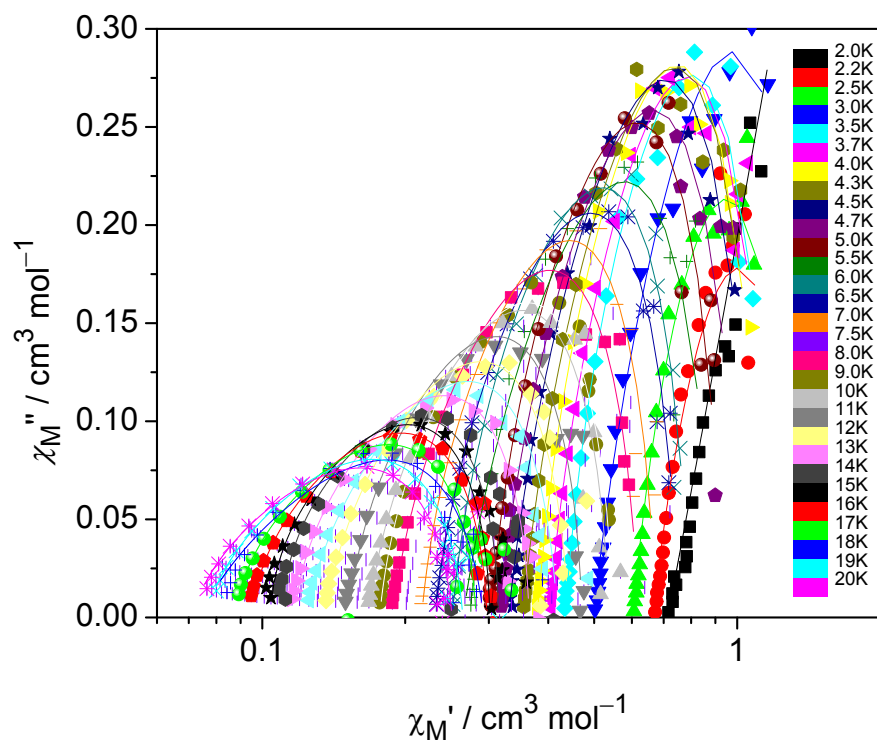


**Figure S10.** Cole Cole plot for **1** from 20 K to 2.0 K.  $H_{dc} = 1.5$  kOe. Solid lines correspond to the best-fit curves.

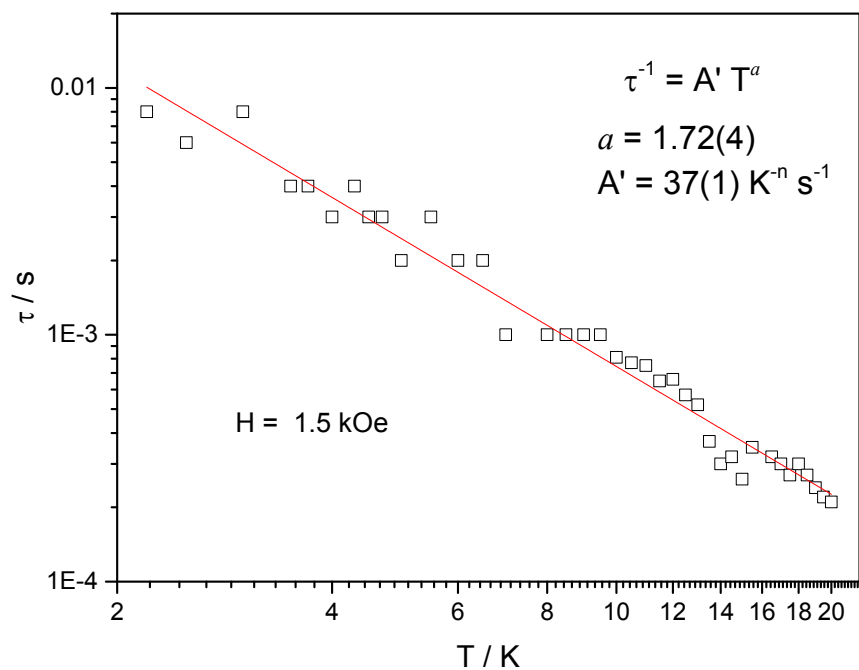


**Figure S11.** Arrhenius plot for **1**. Solid lines represent the best-fit curves. This curve was adjusted considering the bottleneck effect.

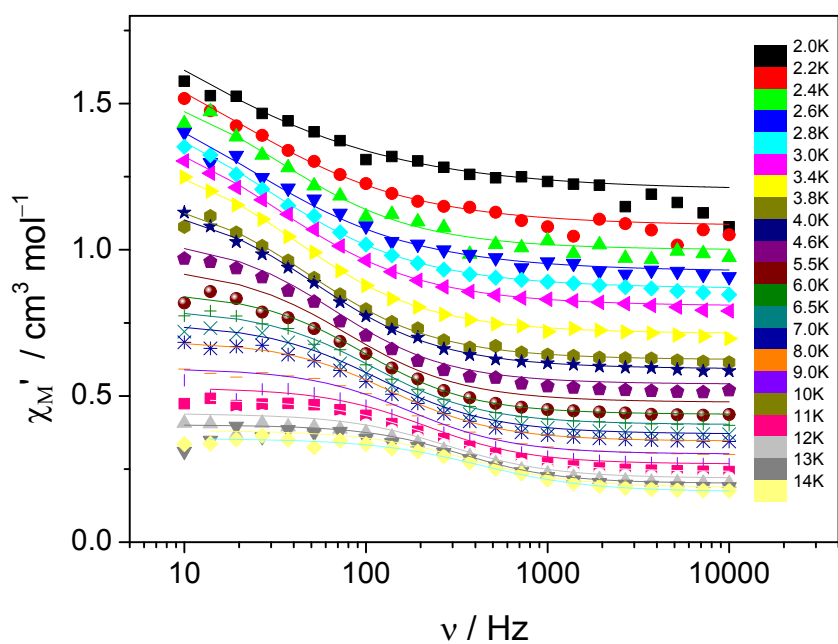


**Figure S12.**  $\chi_M''$  vs.  $\nu$  curves for **1**,  $H_{dc} = 1.0$  kOe, frequency range from 10 Hz to 10 kHz. Solid lines correspond to the best-fit curves according to the generalized Debye model.

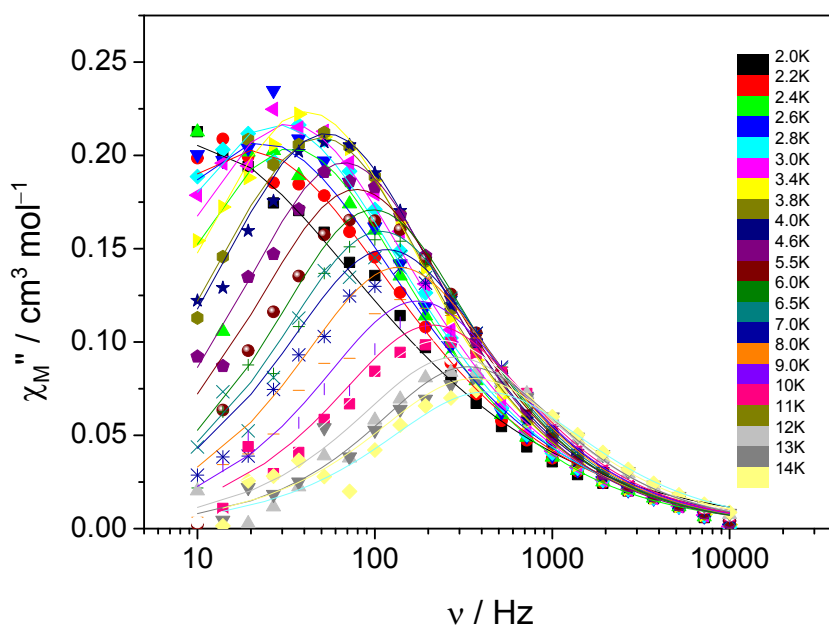


**Figure S13.**  $\chi_M''$  vs.  $\nu$  curves for **1**,  $H_{dc} = 1.0$  kOe frequency range from 10 Hz to 10 kHz. Solid lines correspond to the best-fit curves according to the generalized Debye model.

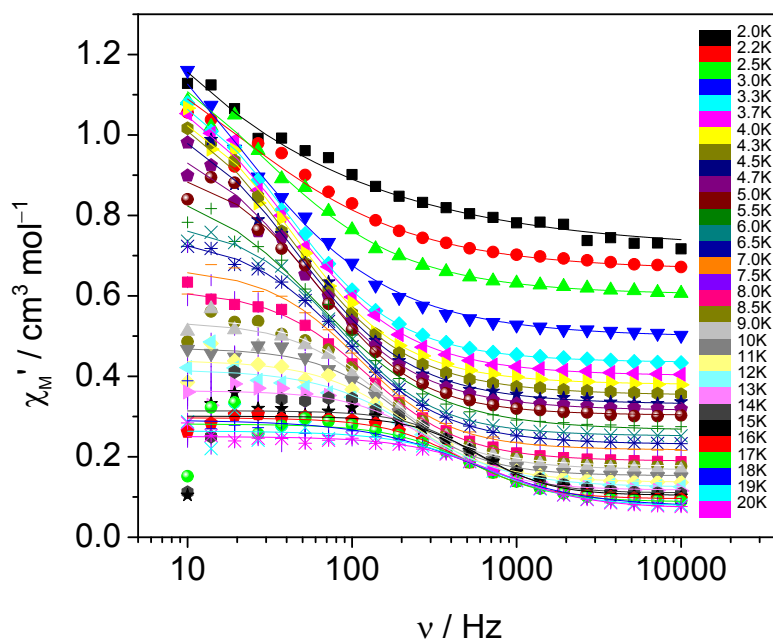


**Figure S14.**  $\chi_M'$  vs.  $\nu$  curves for **1**,  $H_{dc} = 1.5$  kOe frequency range from 10 Hz to 10 kHz. Solid lines correspond to the best-fit curves according to the generalized Debye model.

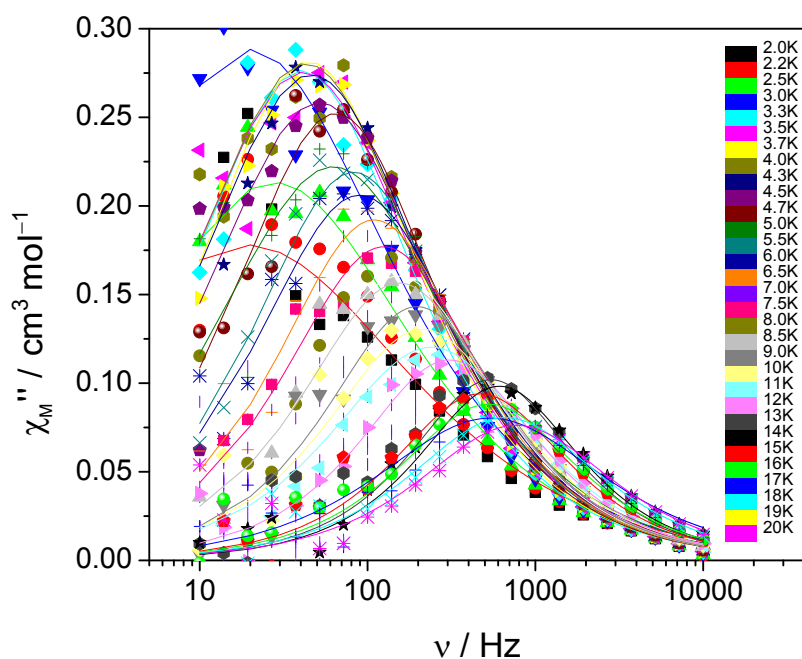


**Figure S15.**  $\chi_M''$  vs.  $\nu$  curves for **1.**  $H_{dc} = 1.5$  kOe frequency range from 10 Hz to 10 kHz. Solid lines correspond to the best-fit curves according to the generalized Debye model.

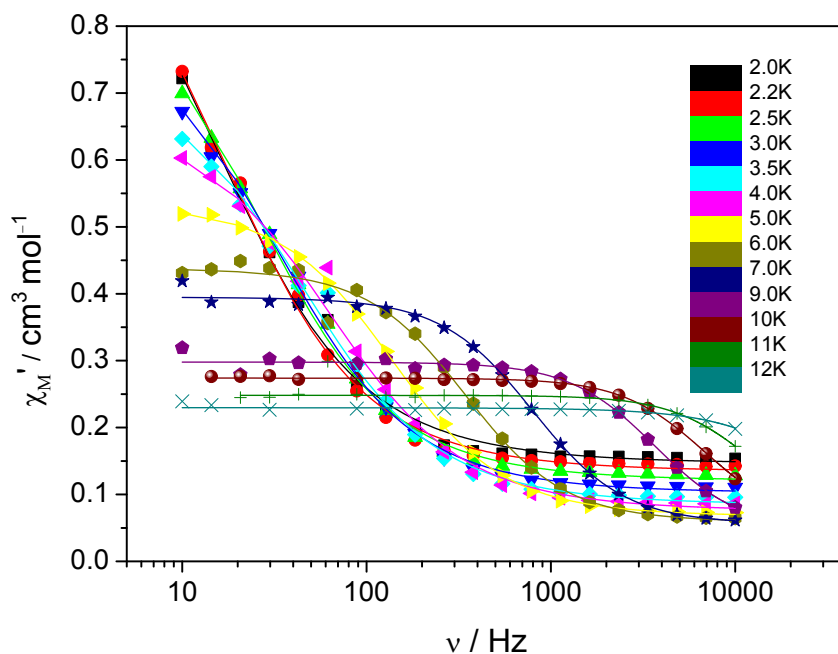


**Figure S16.**  $\chi_M'$  vs.  $\nu$  curves for **2.**  $H_{dc} = 1.0$  kOe frequency range from 10 Hz to 10 kHz. Solid lines correspond to the best-fit curves according to the generalized Debye model.

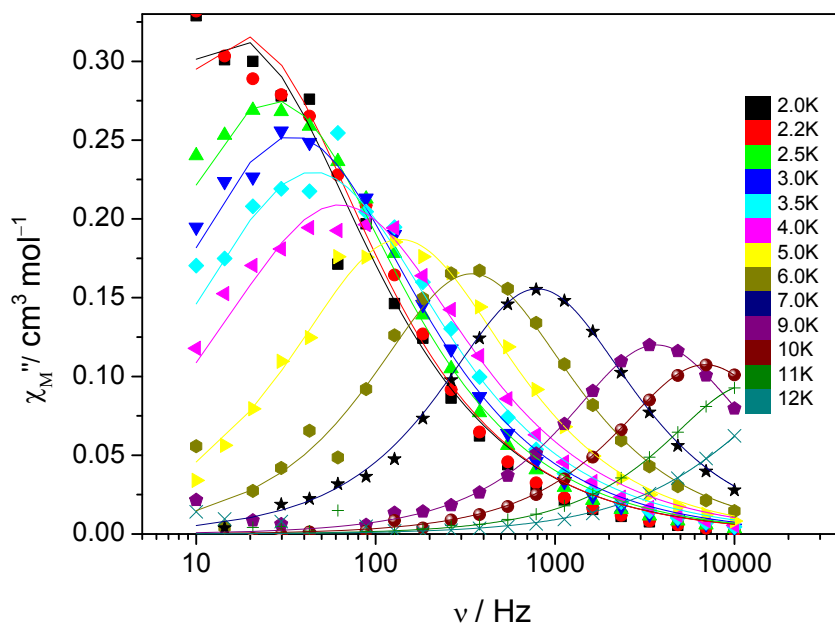


**Figure S17.**  $\chi_M''$  vs.  $\nu$  curves for **2**.  $H_{dc} = 1.0$  kOe frequency range from 10 Hz to 10 kHz. Solid lines correspond to the best-fit curves according to the generalized Debye model.

## References

- (1) da Cunha, T. T.; Barbosa, V. M. M.; Oliveira, W. X. C.; Pinheiro, C. B.; Pedroso, E. F.; Nunes, W. C.; Pereira, C. L. M. Slow Magnetic Relaxation in Mononuclear Gadolinium(III) and Dysprosium(III) Oxamate Complexes. *Polyhedron* **2019**, *169*, 102–113. <https://doi.org/10.1016/j.poly.2019.04.056>.
- (2) CrysAlisPRO. Rigaku Oxford Diffraction: Yarnton, Oxfordshire, E. CrysAlis Pro. Rigaku Oxford Diffraction: Yarnton, England 2018.
- (3) Sheldrick, G. M. XPREP. Bruker-AXS. Madison, Wisconsin, USA 2001.
- (4) Palatinus, L.; Chapis, G. SUPERFLIP – a Computer Program for the Solution of Crystal Structures by Charge Flipping in Arbitrary Dimensions. *J. Appl. Crystallogr.* **2007**, *40* (4), 786–790. <https://doi.org/10.1107/S0021889807029238>.
- (5) Palatinus, L.; Prathapa, S. J.; van Smaalen, S. EDMA : A Computer Program for Topological Analysis of Discrete Electron Densities. *J. Appl. Crystallogr.* **2012**, *45* (3), 575–580. <https://doi.org/10.1107/S0021889812016068>.
- (6) Altomare, A.; Cascarano, G.; Giacovazzo, C.; Guagliardi, A.; Burla, M. C.; Polidori, G.; Camalli, M. SIR 92 – a Program for Automatic Solution of Crystal Structures by Direct Methods. *J. Appl. Crystallogr.* **1994**, *27* (3), 435–435. <https://doi.org/10.1107/S002188989400021X>.
- (7) Sheldrick, G. M. Crystal Structure Refinement with SHELXL. *Acta Crystallogr. Sect. C Struct. Chem.* **2015**, *71* (Md), 3–8. <https://doi.org/10.1107/S2053229614024218>.
- (8) C. K. Johnson. Crystallographic Computing; Ahmed, F.; Hall, S. R.; Huber, C. P., Ed.; Munksgaard: Copenhagen, 1970; pp 207–220.

- (9) Macrae, C. F.; Bruno, I. J.; Chisholm, J. A.; Edgington, P. R.; McCabe, P.; Pidcock, E.; Rodriguez-Monge, L.; Taylor, R.; Van De Streek, J.; Wood, P. A. Mercury CSD 2.0 - New Features for the Visualization and Investigation of Crystal Structures. *J. Appl. Crystallogr.* **2008**, *41* (2), 466–470. <https://doi.org/10.1107/S0021889807067908>.